Available online at www.sciencedirect.com
SCIENCE DIRECT®
Electrochimica Acta 50 (2005) 2125–2134
ELECTROCHIMICA Acta
www.elsevier.com/locate/electacta

Single-ion conducting polymer–silicate nanocomposite electrolytes for lithium battery applications

Mary Kurian[a,1], Mary E. Galvin[a,*], Patrick E. Trapa[b], Donald R. Sadoway[b], Anne M. Mayes[b,2]

[a] *Department of Materials Science and Engineering, University of Delaware, Newark, DE 19716, USA*
[b] *Department of Materials Science and Engineering, Massachusetts Institute of Technology, Cambridge, MA 02139, USA*

Received 28 April 2004; received in revised form 12 September 2004; accepted 13 September 2004

Abstract

Solid-state polymer–silicate nanocomposite electrolytes based on an amorphous polymer poly[$(oxyethylene)_8$ methacrylate], POEM, and lithium montmorillonite clay were fabricated and characterized to investigate the feasibility of their use as 'salt-free' electrolytes in lithium polymer batteries. X-ray scattering and transmission electron microscopy studies indicate the formation of an intercalated morphology in the nanocomposites due to favorable interactions between the polymer matrix and the clay. The morphology of the nanocomposite is intricately linked to the amount of silicate in the system. At low clay contents, dynamic rheological testing verifies that silicate incorporation enhances the mechanical properties of POEM, while impedance spectroscopy shows an improvement in electrical properties. With clay content $\geq$15 wt.%, mechanical properties are further improved but the formation of an apparent superlattice structure correlates with a loss in the electrical properties of the nanocomposite. The use of suitably modified clays in nanocomposites with high clay contents eliminates this superstructure formation, yielding materials with enhanced performance.
© 2004 Elsevier Ltd. All rights reserved.

Keywords: Polymer–silicate nanocomposites; Salt-free nanocomposite electrolytes; Lithium polymer battery; Nanocomposite morphology; Organic silicate modifiers

1. Introduction

The increasing energy needs of modern society have spurred extensive research and development in the areas of energy production, storage and distribution. Devices incorporating solvent-free polymer electrolytes, in particular the 'lithium polymer battery' (LPB), are highly desirable due to characteristics such as inherent low safety risks and their ability to be formed into thin film structures of large surface area, yielding high energy density cells that are lightweight and flexible [1]. However, to realize these performance advantages, several challenges related to materials design must be overcome, including the ability to make LPBs mechanically robust and operable at high current rates while still retaining their lightweight construction. This is particularly important in applications where batteries are designed to serve a secondary function as a structural or insulating element that might commonly encounter significant stress or deformation.

Poly(ethylene oxide) (PEO) doped with alkali metal salts has long been favored a candidate for use as an electrolyte in solid-state rechargeable lithium batteries [2]. However, since the local relaxations and segmental motions of the polymer host that are typically needed [3] to allow efficient Li^+ transport in the electrolyte are best achieved in an amorphous polymer, it is only above the melting temperature of crystalline

* Corresponding author. Tel.: +1 302 831 0873; fax: +1 302 831 4545.
E-mail addresses: megalvin@udel.edu (M.E. Galvin), amayes@mit.edu (A.M. Mayes).
[1] Current address: Air Products and Chemicals, Inc., Corporate Science & Technology Center, 7201 Hamilton Blvd., Allentown, PA 18195, USA.
[2] Tel.: +1 617 253 3318; fax: +1 617 452 3432.

0013-4686/$ – see front matter © 2004 Elsevier Ltd. All rights reserved.
doi:10.1016/j.electacta.2004.09.020

PEO–LiX complexes (∼60 °C) that appreciable conductivities ($\sigma > 10^{-4}$ S/cm) are seen [4]. Most efforts aimed at lowering the operation temperatures of PEO–LiX systems to the ambient region have focused on the development of copolymerization [4–12] or cross-linking [13–17] strategies and the use of suitable plasticizers [1,18,19] to create completely amorphous systems with enhanced conductivity. Incorporation of inorganic particles in the polymer matrix to impart mechanical stability [20], and enhance interfacial properties [21] and conductivity by suppressing crystallization of the PEO host has also been investigated [22–27].

An alternative strategy for creating polymer electrolyte systems with improved electrical and mechanical properties is through fabrication of polymer silicate nanocomposites (PSNs). PSNs are a class of materials in which nanoscale clay particles are molecularly dispersed within a polymer matrix [28–34]. Recent commercial interest in these nanocomposites arises from the fact that they exhibit dramatic increases in tensile strength [30], heat resistance [29] and solvent resistance [35] as well as decreases in gas permeability when compared with the bulk polymer [29]—properties also desirable in electrolytes for LPBs.

Aranda and Ruizhitzky [36] have shown that the incorporation of lithium/sodium montmorillonite clay in a PEO matrix using solution processing results in composite electrolytes with enhanced ionic conductivity in the temperature range 400–700 K. Vaia et al. reported that composite electrolytes with a high inorganic content (60 wt.% clay) fabricated by melt intercalation had higher conductivity (∼10^{-6} S/cm) than $LiBF_4$/PEO electrolytes (∼10^{-8} S/cm) at 30 °C [37]. In most studies, intercalation of the polymer chains in the silicate galleries appears to suppress their tendency to crystallize, resulting in enhanced ionic conductivity. There are also reports of annealing leading to enhanced conductivity due to an increase in PEO intercalation into the clay galleries [38]. Smectic clay/polymer nanocomposites [39] based on [polystyrene/clay] and [poly(methyl methacrylate)-co-acrylamide/clay] prepared by in situ intercalative polymerization of the host polymer in the presence of clay mineral were also studied, but showed very low ionic conductivities. Additionally, gel composite electrolytes [40] of lithium hectorite dispersed in high dielectric solvents (ethylene carbonate and propylene carbonate) exhibited a room temperature conductivity above 10^{-4} S/cm and a transference number of ∼0.8, while PEO intercalated into lithiated taeniolite showed conductivities of 3×10^{-7} S/cm at room temperature [41].

There have also been studies on PSN electrolytes doped with lithium metal salts. [PEO/poly(oxypropylene) diamine modified sodium montmorillonite/$LiCF_3SO_3$] nanocomposites have shown higher ionic conductivities than conventional PEO/LiX electrolytes [42]. Gel electrolytes based on [polyacrylonitrile/organophilic clay/propylene or ethylene carbonate co-solvent/$LiClO_4$] [43] showed an enhancement in dimensional and electrochemical stability due to clay incorporation. However, in these cases, properties were found to be very strongly dependent on clay and co-solvent/plasticizer content.

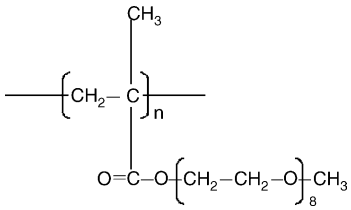

Fig. 1. Schematic representation of structure of poly[(oxyethylene)$_8$ methacrylate] (POEM) polymer.

Our work in this paper reports on the development of "dry" polymer–silicate nanocomposite electrolytes based on a lithium cation exchanged montmorillonite clay (Li-mmt) and an amorphous PEO variant, poly[(oxyethylene)$_8$ methacrylate], POEM, without added plasticizers or dopant salts (Fig. 1 is a schematic representation of the structure of POEM). Here the cations serve as the charge carriers in the PSN electrolyte, while the clay sheets themselves provide immobilized counterions, leading to the formation of a nearly single-ion conductor where the Li^+ transport number should approach a value of unity. Such systems would be expected to hold performance advantages over salt-doped systems at high currents if sufficient conductivities could be achieved [44].

2. Experimental

2.1. POEM synthesis

Poly[(oxyethylene)$_8$ methacrylate] was synthesized by solution-free radical polymerization of the monomer using ethyl acetate as the solvent. Both the OEM monomer (polyethylene glycol methyl ether methacrylate) and the initiator 2,2′-azobisisobutyronitrile (AIBN) were purchased from Sigma-Aldrich and used as received. A clean, dry 500 mL round bottom flask was used as the reactor. Ethyl acetate was introduced into the reactor and monomer was added in the amount that provided a 10% monomer solution. AIBN was added in concentration to yield the desired molecular weight. The reactor was degassed to remove traces of oxygen from the reaction mixture by bubbling argon gas through the mixture for about 15 min, after which the reactor was clamped into an oil bath held at 65 °C. Both the reactants and the oil were stirred individually to achieve good mixing and promote even heating, respectively. The reaction was allowed to proceed for approximately 48 h. The resulting polymer solution was concentrated on a rotary evaporator, precipitated in a hexane–methanol mixture (40:1) and finally dried under vacuum for 24 h to isolate the colorless polymer.

2.2. Clay purification and handling

Sodium montmorillonite (SWy-2, Source Clay Minerals Repository, University of Missouri) was used as the starting

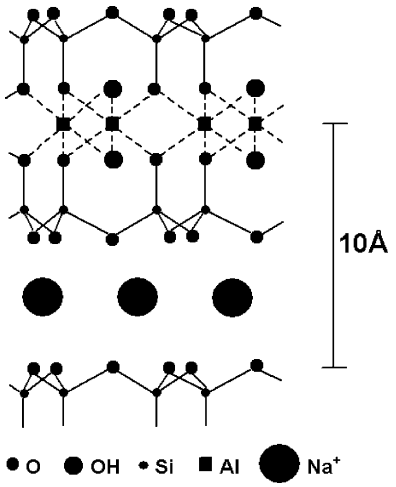

Fig. 2. Schematic representation of the structure of the unit cell in Na^+ montmorillonite clay mineral (adapted from Ref. [45]).

material. Montmorillonite has a net negative charge that is compensated with sodium cations. In the presence of water, the compensating sodium cations on the clay layer surfaces can be easily exchanged for other cations when available in excess amount in solution. (Fig. 2 shows a schematic representation of the unit cell of montmorillonite clay [45] used in this work.)

Prior to use in the nanocomposites, the clay was purified and treated to obtain clean lithium montmorillonite of particle size <2 μm by the following procedure. Twelve grams of sodium montmorillonite were dispersed in 1 L of de-ionized water and the dispersion was allowed to stand for 24 h to allow impurities and heavy mineral fractions to settle. The clean clay suspension was poured into a graduated beaker and the residual heavy sediment was discarded. To ensure complete saturation of the cation exchange capacity positions of the clay with lithium cations, the suspension was saturated with lithium by adding sufficient lithium chloride salt (Fisher Chemicals) to achieve a 1 M solution. (This provides Li^+ in over 100 times excess of the amount required to completely exchange all available cation exchange sites, based on the cation exchange capacity determined for the clay.) The solution was stirred for 24 h to allow for complete replacement of sodium cations by lithium cations and then centrifuged to separate the lithium montmorillonite clay from the supernatant containing the excess ions. The clay was re-suspended in de-ionized water and stirred for 12 h to remove excess ions. This suspension was then re-centrifuged to recover the clay. The conductivity of the supernatant was monitored and the clay was repeatedly washed, centrifuged and separated till the supernatant showed no further decrease in conductivity, indicating the removal of all excess cations from the clay [45]. The purified and exchanged clay was freeze-dried for a week to remove all traces of water which could be adsorbed on the clay layers and possibly interfere with the battery performance in the applications we seek to investigate. The dried clay was then powdered using a mortar and pestle.

Table 1
Sample nomenclature and estimated [Li^+:EO] ratios for POEM–Li^+ montmorillonite nanocomposite electrolytes

Sample	Composition [Li-clay/POEM] (w/w)	Estimated [Li^+:EO] ratio
2%_PSN	2/98	7×10^{-4}
5%_PSN	5/95	1.8×10^{-3}
10%_PSN	10/90	3.9×10^{-3}
15%_PSN	15/85	6.1×10^{-3}
20%_PSN	20/80	8.8×10^{-3}
25%_PSN	25/75	11.6×10^{-3}

2.3. Nanocomposite fabrication

A solution technique using dry, distilled acetonitrile as solvent was employed in all of the nanocomposite preparations. All nanocomposite handling was done inside an argon-filled glove box (moisture and oxygen levels were measured to be less than 1 ppm) to maintain dry conditions and avoid contamination of the electrolytes. POEM/lithium montmorillonite nanocomposites with 2, 5, 10, 15, 20 and 25 wt.% of clay were prepared (Table 1 lists sample nomenclature used in this report). Measured amounts of POEM and Li-mmt were each dissolved separately in 250 mL acetonitrile and stirred for 24 h. The polymer solution was then added to the clay suspension with rapid stirring to ensure maximum contact between the polymer chains and clay platelets. This mixed solution was stirred for 24 h, after which it was evaporated to dryness on a rotary evaporator. The composite was further dried under vacuum at 60 °C for 24 h.

2.4. Preparation of organically modified Li-mmt and fabrication of the corresponding nanocomposites

A simple solution technique was used to modify Li-mmt using diamine-terminated PEO, $[NH_2]_2$-PEO (Scientific Polymer Products, Inc., molecular weight ∼2000 g/mol, amine content ∼0.88 meq/g). A measured amount of Li-mmt was dispersed in de-ionized (DI) water and the solution was allowed to stir for 12 h. In a similar manner, the modifier solution was made by dissolving a calculated amount of $[NH_2]_2$-PEO separately in DI water and allowing it to stir for 12 h. The modifier solution was then added to the clay dispersion and the mixed solution stirred for a further 12 h. Two different modified clay solutions were made based on the extent of modification of the clay by the organic modifier, the first such that only 10% of the cation exchange sites were modified (∼2 wt.% $[NH_2]_2$-PEO) and the second with 50% of the sites modified (∼11 wt.% $[NH_2]_2$-PEO). Solutions of measured amounts of the matrix polymer POEM were also made in DI water. The polymer solution was then added to a measured amount of the clay suspension with rapid stirring to ensure maximum contact between the polymer chains and clay platelets. This mixture was stirred for 24 h, after which it was evaporated to dryness on a rotary evaporator and further dried under vacuum at 60 °C for 24 h. Two sets of composites,

each incorporating PSNs with 10, 15 and 20 wt.% clay, were made using the two different organically modified clays.

3. Characterization

The cation exchange capacity for the native sodium montmorillonite clay and the exchanged lithium montmorillonite were determined using standard soil chemical analysis techniques [46–48].

As described in the experimental procedures, all nanocomposite fabrication and handling was done in the controlled atmosphere of an argon-filled glove-box (moisture and oxygen levels were measured to be less than 1 ppm), since residual water in the electrolytes would greatly affect the ionic conductivity of the electrolytes. Thermogravimetric analysis (TGA) was used to verify that the nanocomposites were completely dry and moisture-free. A sample 5–10 mg in weight was analyzed using a Perkin Elmer TGA 7 instrument by recording the weight loss of the sample as a function of temperature in the range 30–900 °C. The presence of water in the sample can be determined by the weight loss at 100 °C, while the amount of residue that remains at the end of the experimental run provides a measure of the inorganic or ash content in the material.

Small angle X-ray scattering (SAXS) was used to monitor the gallery height of lithium montmorillonite in the different nanocomposites. Room temperature scans were collected in transmission mode using a Rigaku Rotoflex diffractometer (Rigaku/USA Inc.), equipped with a rotating anode X-ray generator (operated at a 30 kV–100 mA setting) with a Cu target and a Bruker 2D area detector (Bruker Analytical X-ray Systems). Samples (5 mm diameter, 2 mm thick), sandwiched using Kapton* polyimide film tape (Precision PCB Services, Inc.) were mounted on a custom-made vertical sample positioning stage situated in an evacuable beam path to reduce background scattering due to air. Background subtractions were made for all sample spectra.

Transmission electron microscopy (TEM) was used to directly observe the nanocomposite morphology. Since POEM has a low $T_g \sim -65$ °C, sections were microtomed from bulk samples under cryogenic conditions using a Leica Ultracut ultramicrotome (Leica Inc.). Sections ~50 nm thick were mounted on 1000 mesh carbon coated grids (Ted Pella Inc.) for observation. Microscopy was performed on a JEOL 2010F TEM, operated at an accelerating voltage of 200 kV.

Electrical conductivities of the PSNs were measured by impedance spectroscopy using a Solatron 1260 impedance gain/phase analyzer (Solatron Instruments, Allentown, PA). The nanocomposite electrolytes were placed between a pair of blocking electrodes made of 316 stainless steel and pressed to a thickness of 250 μm. The electrode assembly was then placed inside a brass cell equipped with seven hermetically sealed ports. To maintain dry conditions, the sample preparation was carried out in an argon-filled glove box (moisture level measured to be less than 2 ppm). Two ports, equipped with valves, served as inlet and outlet for argon or nitrogen flow. The last port accommodated an O-ring sealed glass tube through which a type-K thermocouple was fed and positioned directly next to one of the stainless steel electrodes. The use of compression fittings rendered the cell cap vacuum tight. The sealed cell was removed from the glove box and annealed at 70 °C for 12 h, blanketed by a continuous flow of dry, grade 5.0 argon. Conductivity measurements were carried out over a temperature interval spanning 20–70 °C. The specimen was protected at all times during the experiment by flowing dry nitrogen gas.

Lithium symmetric cells fitted with the PSN electrolytes were used to obtain a measure of lithium transference number. The electrodes were active to lithium ions but blocked the anions; upon application of a stepped potential, the initial current (I_0) reflected both cation and counter ion contributions whereas the long-term, steady-state value (I_{ss}) arose solely from lithium ion motion. The transference number was then taken to be I_{ss}/I_0.

To determine the effect of clay content on the mechanical performance of the PSN electrolytes, rheological characterization was performed using an ARES rheometer (Rheometrics, Inc.) with a parallel plate fixture. Temperature was maintained at 25 °C during the measurements using a Peltier system. Samples were pressed to a gap width of 1 mm under a stable normal force of approximately 100 g. The complex shear modulus, $G = G' + iG''$, was measured as a function of frequency by dynamically shearing the sample at a fixed strain rate over the low frequency regime 0.1–10 rad/s.

4. Results and discussion

The molecular weight and polydispersity of the synthesized POEM polymer were measured to be approximately 100 kg/mol and 2.1, respectively, by gel permeation chromatography using polystyrene calibration standards. The glass transition temperature (T_g) was determined by differential scanning calorimetry (DSC) to be -65 ± 5 °C.

The cation exchange capacity (CEC) of the clay was determined to be 67 meq/100 g clay using standard soil chemical analysis techniques [46–48]. Since these values are fairly dependent on the exact technique and soil handling method used, we can consider it to be in good agreement with the manufacturer's reported value of 77 meq/100 g clay. We use the measured value of the CEC in all relevant calculations.

TGA results for the nanocomposite electrolytes showed no detectable weight loss that could be associated with the presence of either residual water or organic solvents from the fabrication techniques used, thus confirming that the materials are "dry" and measured materials properties are not influenced by such contaminations. A nanocomposite with 2 wt.% clay exhibited a decomposition temperature of 400 °C, roughly 50 °C above that of neat POEM.

X-ray diffraction is an ideal tool to study the structure of clay minerals [49]. In order to monitor the interactions of

the silicate with the polymer, the gallery height of the clay was measured as a function of POEM content. SAXS plots of intensity versus angle of scattering, 2θ, for the neat clay and the different nanocomposites, along with corresponding *d*-spacings, are shown in Fig. 3.

These results give direct evidence of the formation of intercalated morphologies in the PSNs. There is an increase in the spacing of (0 0 1) planes from about 10 Å in the native lithium montmorillonite clay to between 17 and 18 Å in the 2, 5, and 10 wt.% clay nanocomposites due to favorable interactions between the polar polymer molecules and the hydrophilic silicate sheets. This primary spacing is similar to values seen in other reports, obtained for the intercalation of PEO into layered silicates [36,37,50–53]. With 15 wt.% or more clay incorporation, a second peak appears at $2\theta \sim 2.8^\circ$ corresponding to a *d*-spacing of about 31 Å. These results suggest the formation of a superlattice structure of tactoids containing two silicate layers at higher clay loadings. Ogata et al. [54] observed a similar low angle peak in studies of PEO-intercalated montmorillonite containing 5–15 wt.% organo-modified clay. In their case, the corresponding long period was ~70 Å, suggesting a possible superlattice arrangement of 4-layer tactoids [54]. Hence at higher clay loadings, bundles of sheets, which are approximately 100–200 nm in lateral dimension, apparently interact to form a superstructure.

Sample	$2theta_1$ (°)	$2theta_2$ (°)	d_1 (Å)	d_2 (Å)
Li-mmt	8.6	-	10.3	-
2%_PSN	4.9	-	18	-
5%_PSN	5.1	-	17.3	-
10%_PSN	5.1	-	17.3	-
15%_PSN	5.2	2.8	17	31.6
20%_PSN	5.2	2.9	17	30.5
25%_PSN	5.1	2.8	17.3	31.6

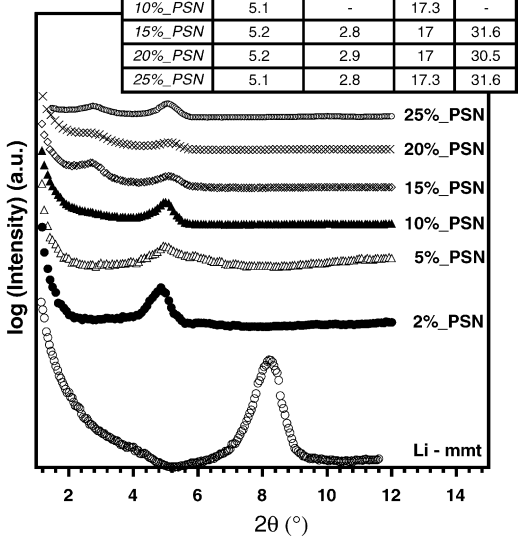

Fig. 3. Room temperature X-ray scattering data for POEM–Li^+ montmorillonite nanocomposites.

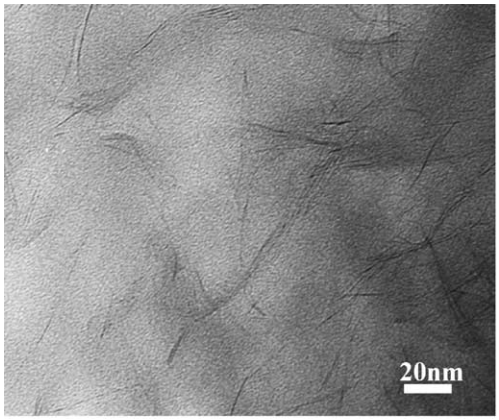

(a) PSN with 5wt% clay content

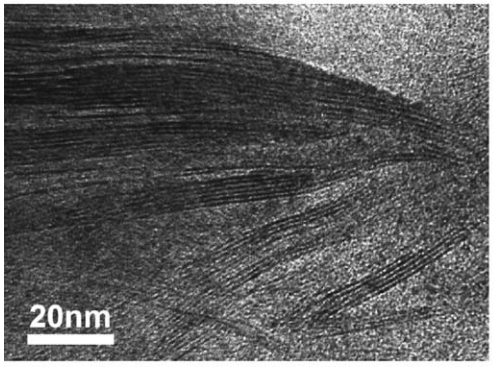

(b) PSN with 15wt% clay content

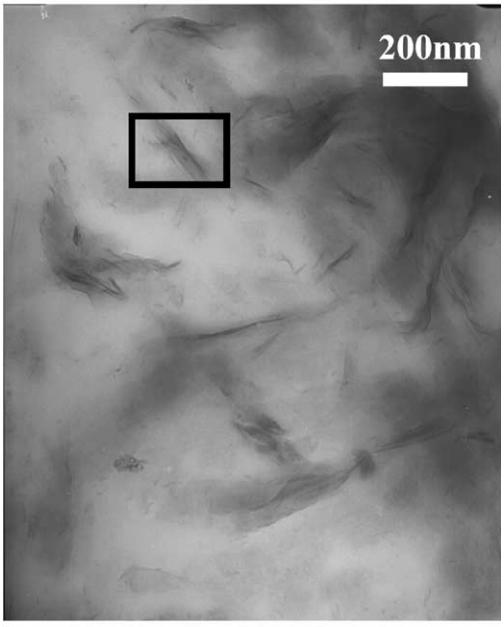

(c) PSN with 15wt% clay content

Fig. 4. TEM micrographs for POEM–Li^+ montmorillonite nanocomposites with different clay loadings: (a) low (5 wt.%) clay content, (b) and (c) high (15 wt.%) clay content.

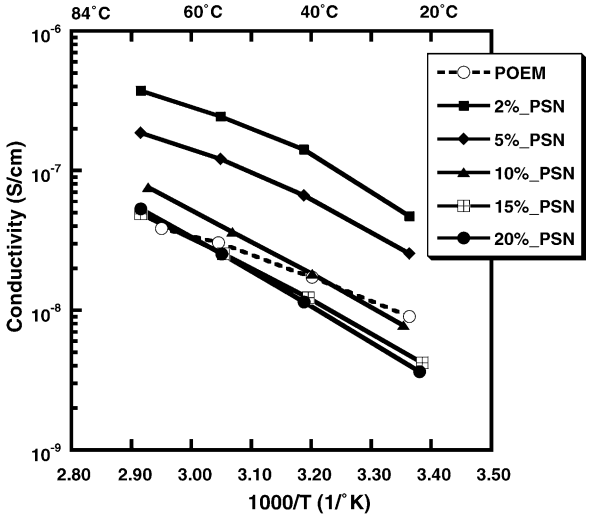

Fig. 5. Temperature dependence of electrical conductivity for POEM–Li^+ montmorillonite nanocomposites of varying clay content.

TEM micrographs yield more information about the morphologies formed in the nanocomposite electrolytes. Representative micrographs for the nanocomposites incorporating low (5 wt.%) and high (15 wt.%) clay contents are shown in Fig. 4. At lower clay loadings (Fig. 4(a)), in addition to intercalated regions, the presence of a significant number of individual delaminated clay platelets dispersed homogeneously in the polymer matrix indicates that some exfoliation has occurred in the nanocomposites. In contrast, at higher loadings, a limited number of exfoliated clay sheets are seen, but more prominently, bundles of intercalated tactoids (Fig. 4(b)) are non-homogeneously dispersed in the polymer matrix (Fig. 4(c)), indicating a tendency towards possible phase separation. The formation of such phase-separated materials at intermediate polymer contents is consistent with recent studies by Shen et al. [55] on the saturation limit of PEO in montmorillonite clay. These authors observed intercalation of up to 28 wt.% PEO in montmorillonite. For higher polymer contents, a PEO-rich phase was also observed.

Measured values of the electrical conductivities for the PSN electrolytes in the temperature range 20–70 °C, are shown in Fig. 5. The results show that there is up to an order of magnitude increase in conductivity of neat POEM with the addition of 2 and 5 wt.% clay, the highest value of 3.75×10^{-7} S/cm being obtained in the former case at a temperature of 70 °C. At 10 wt.% clay incorporation, the composite performs better than neat POEM at higher temperatures (>40 °C) but its performance decays to below that of POEM at lower temperatures. With 15 wt.% and higher clay content (conductivity data for the 20 and 25 wt.% PSNs were identical), the conductivities fall to lower values, distinctly below that of the neat polymer.

As discussed in the scattering analysis, there seems to be a transition in the morphology associated with systems incorporating ≥15 wt.% clay, which may account for the decay in electrical properties. Discrepancies between the shape of the impedance spectra of the low and high clay-content PSNs (Fig. 6) suggest that different conduction mechanisms are present in the two electrolytes. Data obtained from the 2 wt.% clay sample appear semicircular (Fig. 6(a)), and can be fit well using a common equivalent circuit consisting of a resistor and capacitor in parallel. In contrast, the spectrum for the 25 wt.% clay electrolyte exhibits a depressed semicircle (Fig. 6(b)), characteristic of a system where more than one conduction process is present simultaneously. TEM micrographs show that, at higher clay loading, uniform dispersion of the clay in the POEM matrix is more difficult to achieve, leading to the formation of phase-separated morphologies. This is expected to affect the conductivity of the system, since the Li^+ carriers are no longer uniformly distributed throughout the material. Moreover, the clay platelets could be acting as physical barriers to the effective motion of carriers, thus leading to a decrease in conductivity of the electrolyte below that of POEM.

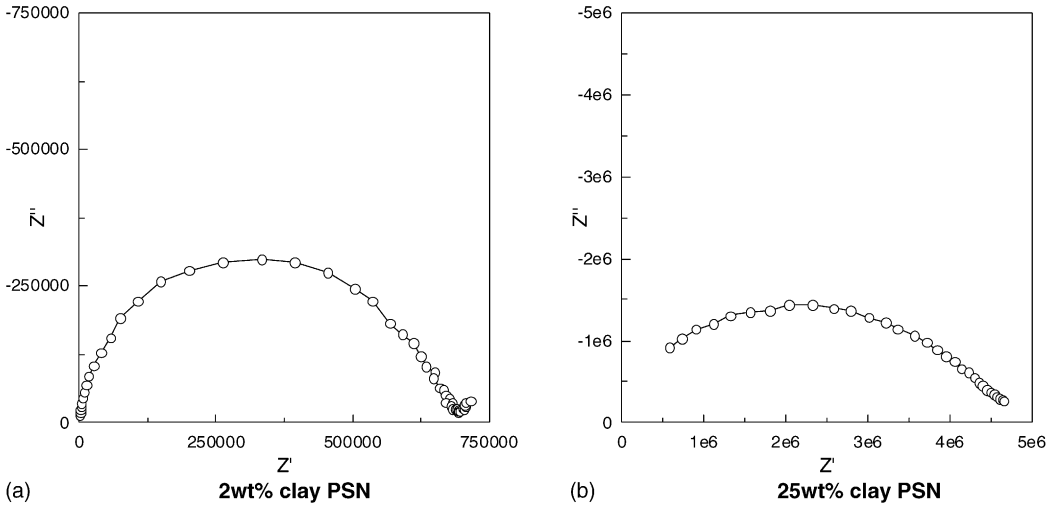

Fig. 6. Impedance plots at 70 °C for PSNs with: (a) 2 wt.% clay and (b) 25 wt.% clay content.

Evidence for single-ion conduction in these PSN electrolytes was obtained from transference number measurements. For example, in measurements of the 2 wt.% clay nanocomposite electrolyte using a symmetric lithium cell, the application of a stepped potential led to a simultaneous jump in the current that was subsequently maintained. Less than 1% current decay was observed, indicating that anions were effectively immobile over the course of the measurement, yielding $I_{ss}/I_0 = t_{Li^+} \sim 1$. To confirm that this current arose from ionic rather than electronic processes, a second stepped potential measurement using stainless steel blocking electrodes was performed, which resulted in a 92% current decay arising from the blocking of Li^+ motion at the electrodes, demonstrating that the majority of the current is carried by these ions. Hence these materials can be viewed as single-ion conductors.

Conductivities between 10^{-4} and 10^{-5} S/cm have been reported for [clay/PEO] [36] nanocomposites (70–75 wt.% clay, 250 °C). [PEO/NH_4^+ smectic] [50] composites with similarly high inorganic contents had a conductivity $\sim 10^{-7}$ S/cm in the temperature range 125–280 °C, while other [clay/polymer] systems [39] exhibited conductivities in the range of 10^{-8} to 10^{-10} S/cm (10 wt.% clay, 85–110 °C). Others report conductivities of 1.6×10^{-6} S/cm (60 wt.% clay, 30 °C) [37] and 10^{-5} S/cm (75 wt.% clay, RT) [38] for [PEO/clay] nanocomposites. As can be seen from the preceding discussion, other studies dealing with similar "dry" electrolyte systems incorporate significantly higher amounts of clay (60–70 wt.%) and hence a larger concentration of carriers in comparison with the current system under consideration. Most of these studies also measure conductivities at much higher temperatures. Though the highest values of conductivity reported herein are low in comparison with many PEO-based electrolytes reported in the literature, it must be noted that the systems described in this work are salt-free and much lower in [Li^+:EO] ratios (Table 1). Further work is needed to assess the promise of these systems as battery electrolytes, focusing on the development of oriented morphologies with a higher [Li^+:EO] ratio.

Given the low glass transition temperature ($T_g \sim -65$ °C) of the POEM matrix and the resulting 'gel' like nature of the nanocomposites at room temperature [56], one of the best methods of characterizing the mechanical behavior of this system is through rheological measurements. Fig. 7 shows plots of the complex moduli for POEM and the nanocomposites as a function of frequency in the low frequency regime. Rheological studies indicate an enhancement in the

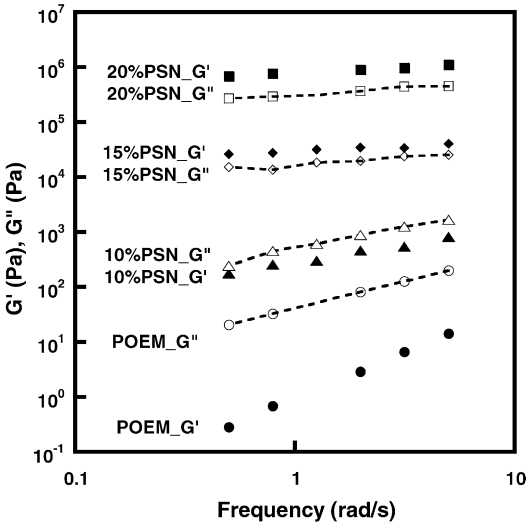

Fig. 7. Room temperature complex moduli for POEM and nanocomposites.

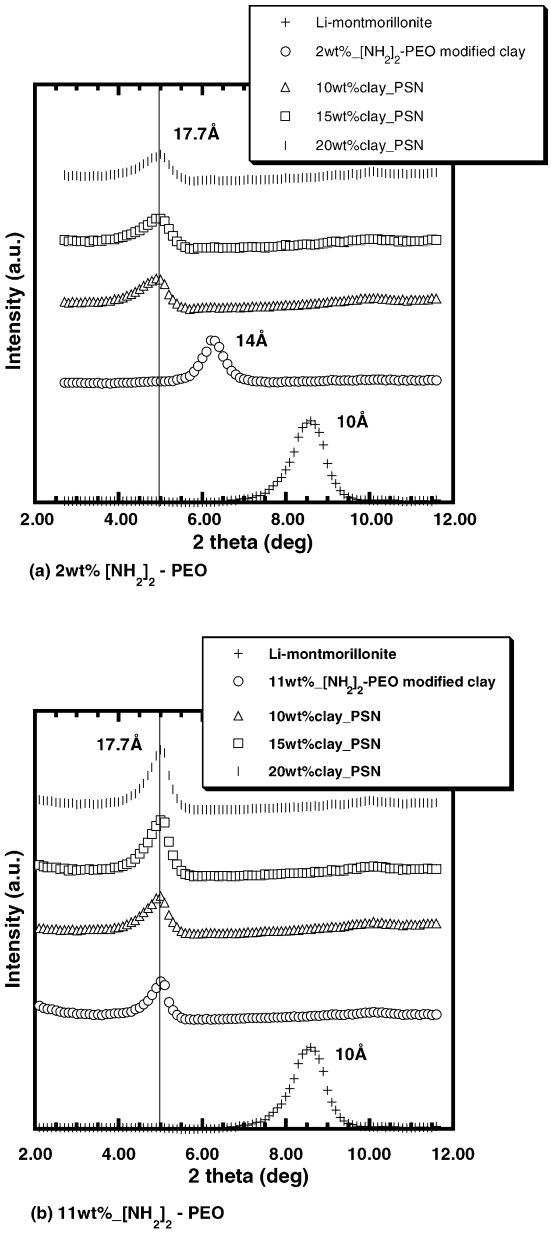

Fig. 8. Room temperature X-ray scattering data for POEM/Li-montmorillonite nanocomposites fabricated using clays modified to different extents with diamine-terminated PEO.

mechanical properties of POEM with the incorporation of clay. We observe an increase in the complex modulus with increasing clay content by up to six orders of magnitude at a loading of 20 wt.%. The loss modulus G'' is greater than the storage modulus G' at lower clay loadings, with a reversal in the trend at higher ($\geq$15 wt.% clay) loadings. This reversal, indicative of a switch from liquid-like to solid-like behavior, is expected with increasing clay content. It is interesting to note that in these measurements too, the transition in the mechanical behavior of the PSNs is strongly linked to the clay content and occurs at 15 wt.% clay loading, similar to the morphological and electrical characteristics. The rheology resembles that exhibited by a strongly gelled pseudo-solid network [57]. The moduli are fairly constant in the frequency regime employed and the small slope of the curves is indicative of the high strength of the composites.

From the above findings, the electrolyte properties appear closely linked with clay content. At higher loadings, the clay is non-uniformly dispersed in the matrix and may form physical barriers to the motion of the charge carriers. In an attempt to promote more uniform dispersion of the clay at higher loadings, nanocomposites incorporating organically modified Li-mmt were fabricated, where the modification of the clay is expected to aid its dispersion in the POEM matrix. Two sets of nanocomposites incorporating clay modified with diamine-terminated PEO to different extents (2 and 11 wt.%) were made. For each set, PSNs with clay contents of 10, 15, 20 wt.% were fabricated.

SAXS data for the two modified clays and the corresponding sets of PSNs are shown in Fig. 8(a) and (b). The data exhibit a single reflection corresponding to a spacing of about 17.7 Å, slightly larger than the spacing for nanocomposites prepared with unmodified clay at the same loading. Fig. 9 compares the scattering data for a representative nanocomposite incorporating unmodified clay (15 wt.% clay) with PSNs having similar inorganic contents but incorporating clay modified to different extents with $[NH_2]_2$-PEO. The use of $[NH_2]_2$-PEO modified clay appears to disrupt the superlattice structure seen for the unmodified system, as evidenced by the disappearance of the low angle reflection at 2.8°. The results indicate that incorporation of $[NH_2]_2$-PEO in the PSNs improves the dispersion of the clay platelets in the POEM matrix, yielding morphologies similar to those observed at lower clay loadings in unmodified PSNs.

The change in morphology due to clay modification has a corresponding effect on the electrical properties of the material. Electrical conductivities for the $[NH_2]_2$-PEO modified

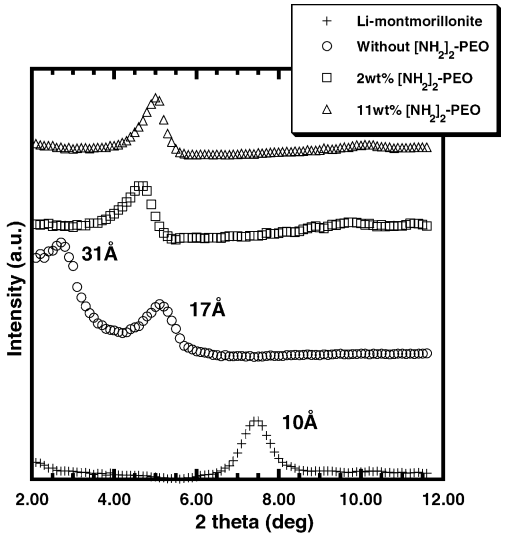

Fig. 9. X-ray scattering data for PSNs (15 wt.% clay content)—use of unmodified clay vs. clay modified to different extents with diamine-terminated PEO.

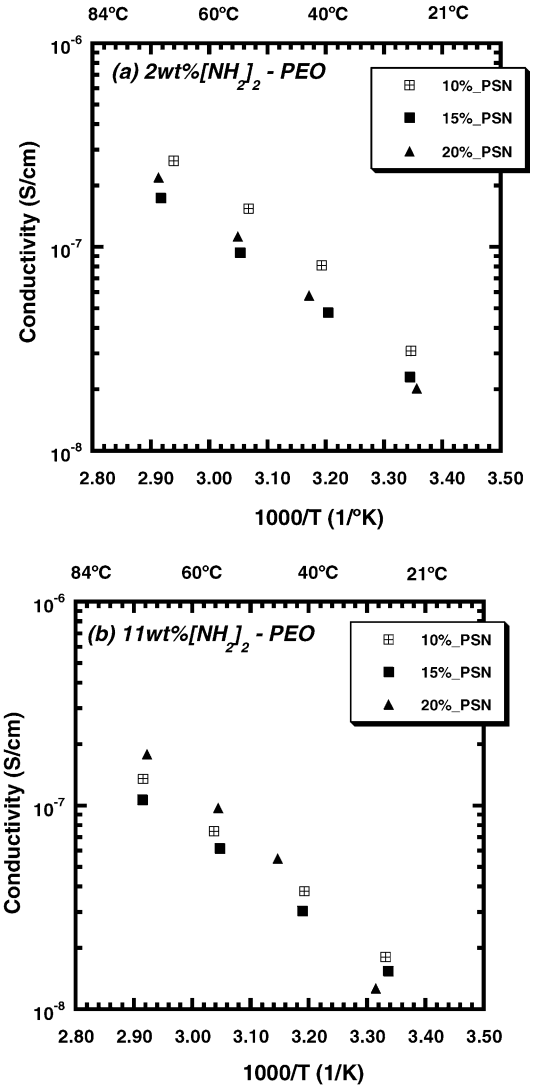

Fig. 10. Temperature dependence of electrical conductivity for POEM/Li-montmorillonite PSNs fabricated using clays modified by diamine-terminated PEO: (a) clay modified with 2 wt.% $[NH_2]_2$-PEO; (b) clay modified with 11 wt.% $[NH_2]_2$-PEO.

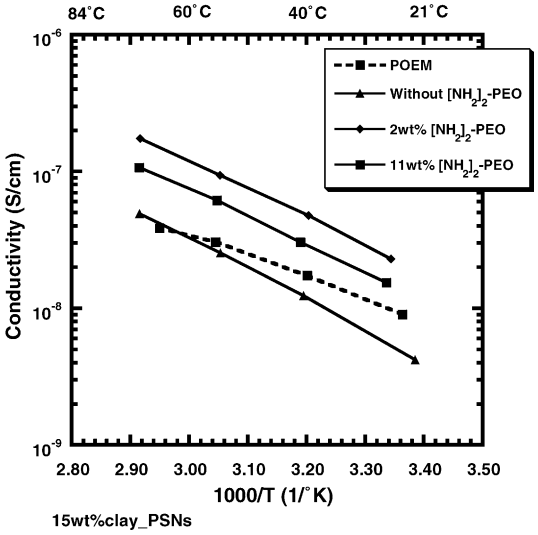

Fig. 11. Temperature dependence of electrical conductivity for PSNs (15 wt.% inorganic content)—use of unmodified clay vs. clay modified to different extents with diamine-terminated PEO.

clay PSNs, measured by impedance spectroscopy are shown in Fig. 10(a) and (b). Compared with the PSNs incorporating unmodified clay, an increase in conductivity is seen with the use of modified clays. Representative data for nanocomposites incorporating 15 wt.% clay are shown in Fig. 11, where electrical conductivities for 15%_PSN (*unmodified clay*) and POEM, are contrasted with the conductivities for 15%_PSN (*2 wt.% $[NH_2]_2$-PEO*) and 15%_PSN (*11 wt.% $[NH_2]_2$-PEO*). Similar behavior is seen for the 10 and 20 wt.% clay systems. Inspection of these results indicates no systematic trend in the electrical properties with clay content. It is expected that properties would depend on both the extent of modification of the silicate by the organic modifier, as well as the subsequent level of clay loading in the nanocomposite. It should be noted that the two levels of modification of the clay by the diamine-terminated PEO modifier (*2 wt.% $[NH_2]_2$-PEO*, i.e. exchange of 10% of CEC, and *11 wt.% $[NH_2]_2$-PEO*, i.e. exchange of 50% of CEC), were chosen arbitrarily and no attempt was made to optimize the level of modification. The results seen here could indicate that there exists an optimal level of organic modification of the clay with regard to electrical properties.

Transference number measurements on the modified clay PSNs gave similar results to those obtained for the 'unmodified' clay/POEM nanocomposites, with Li^+ carriers accounting for ~90% of the current, and the rest arising from electronic processes.

The use of modified clays also enhanced the mechanical properties of the PSNs beyond those of the unmodified clay systems. Attempts to quantify the mechanical properties of modified clay nanocomposites with dynamic rheological measurements in the frequency range used for the unmodified clay PSNs were unsuccessful due to the more solid-like nature of these systems. While higher temperatures could be employed for such measurements, we did not undertake them here due to concerns over thermal degradation.

5. Conclusions

Solid-state electrolytes based on polymer–silicate nanocomposites have been fabricated using an amorphous PEO-based polymer, POEM, and lithium montmorillonite clay. The incorporation of the silicate in the POEM matrix leads to a considerable enhancement in mechanical properties. Scattering studies indicate that the nanocomposites primarily exhibit an intercalated morphology with the formation of an apparent superlattice structure at higher clay contents. At lower loadings, TEM results suggest the clay is more homogeneously distributed in the matrix in comparison with higher clay loadings. The presence of completely exfoliated sheets at lower loadings indicates that partial exfoliation has occurred in these materials, whereas at higher loadings, non-uniformly distributed intercalated tactoids are more predominant. Partial modification of the clay by an organic modifier appeared to aid the dispersion of the clay at higher loadings, consequently enhancing electrical performance. The effect of the level of modification of the clay on electrical properties, though not explicitly investigated in the current report, could be an important parameter, which could be controlled to create electrolytes with optimal properties.

Although electrical conductivities of the PSNs investigated in this work are low in comparison with conventional polymer electrolytes, these materials are salt-free and incorporate significantly lower lithium ion concentrations. We expect that the formation of a fully exfoliated system, perhaps through the use of shear, would lead to improved electrical properties, as would the use of clays having higher cation exchange capacities and hence Li^+ concentration.

Acknowledgments

The authors thank Dr. Chaoying Ni and Mr. Frank Kriss from the W.M. Keck Electron Microscopy Facility at the University of Delaware for their help with transmission electron microscopy studies and Dr. Sudhir Shenoy for assistance with the rheological experiments. M.K. gratefully acknowledges partial funding by the University of Delaware Competitive Fellowships. This work was sponsored by the Office of Naval Research through Grants N00014-00-1-0356 and N00014-02-1-0226.

References

[1] F.M. Gray, Solid Polymer Electrolytes: Fundamentals and Technological Applications, VCH Publishers, Inc., New York, 1991.
[2] P. Lightfoot, M.A. Mehta, P.G. Bruce, Science 262 (1993) 883.

[3] F. Chia, Y. Zheng, J. Liu, N. Reeves, G. Ungar, P.V. Wright, Electrochim. Acta 48 (2003) 1939.
[4] D. Fauteux, A. Massucco, M. McLin, M. Vanburen, J. Shi, Electrochim. Acta 40 (1995) 2185.
[5] P.P. Soo, B.Y. Huang, Y.I. Jang, Y.M. Chiang, D.R. Sadoway, A.M. Mayes, J. Electrochem. Soc. 146 (1999) 32.
[6] H.R. Allcock, P.E. Austin, T.X. Neenan, J.T. Sisko, P.M. Blonsky, D.F. Shriver, Macromolecules 19 (1986) 1508.
[7] K.M. Abraham, M. Alamgir, S.J. Perrotti, J. Electrochem. Soc. 135 (1988) 535.
[8] J.S. Tonge, D.F. Shriver, J. Electrochem. Soc. 134 (1987) 269.
[9] D.W. Xia, J. Smid, J. Polym. Sci. Polym. Lett. 22 (1984) 617.
[10] J.M.G. Cowie, R. Ferguson, J. Polym. Sci. Polym. Phys. 23 (1985) 2181.
[11] J.M.G. Cowie, A.C.S. Martin, Polym. Commun. 26 (1985) 298.
[12] F.M. Gray, J.R. Maccallum, C.A. Vincent, J.R.M. Giles, Macromolecules 21 (1988) 392.
[13] J.R. Maccallum, M.J. Smith, C.A. Vincent, Solid State Ionics 11 (1984) 307.
[14] M. Watanabe, S. Nagano, K. Sanui, N. Ogata, Polym. J. 18 (1986) 809.
[15] M. Andrei, L. Marchese, A. Roggero, P. Prosperi, Solid State Ionics 72 (1994) 140.
[16] A. Killis, J.F. Lenest, H. Cheradame, A. Gandini, Makromol. Chem. 183 (1982) 2835.
[17] H. Cheradame, J.F. LeNest, in: J.R. Maccallum, C.A. Vincent (Eds.), Polymer Electrolyte Reviews, vol. 1, Elsevier, London, 1987, p. 103.
[18] K.M. Abraham, in: B. Scrosati (Ed.), Applications of Electroactive Polymers, Chapman & Hall, London, 1993, p. 75.
[19] I.E. Kelly, J.R. Owen, B.C.H. Steele, J. Power Sources 14 (1985) 13.
[20] J.E. Weston, B.C.H. Steele, Solid State Ionics 7 (1982) 75.
[21] F. Capuano, F. Croce, B. Scrosati, J. Electrochem. Soc. 138 (1991) 1918.
[22] F. Croce, G.B. Appetecchi, L. Persi, B. Scrosati, Nature 394 (1998) 456.
[23] F. Croce, R. Curini, A. Martinelli, L. Persi, F. Ronci, B. Scrosati, R. Caminiti, J. Phys. Chem. B 103 (1999) 10632.
[24] W. Wieczorek, Z. Florjanczyk, J.R. Stevens, Electrochim. Acta 40 (1995) 2251.
[25] W. Krawiec, L.G. Scanlon, J.P. Fellner, R.A. Vaia, E.P. Giannelis, J. Power Sources 54 (1995) 310.
[26] A.S. Best, A. Ferry, D.R. MacFarlane, M. Forsyth, Solid State Ionics 126 (1999) 269.
[27] C. Capiglia, P. Mustarelli, E. Quartarone, C. Tomasi, A. Magistris, Solid State Ionics 118 (1999) 73.
[28] K. Yano, A. Usuki, A. Okada, T. Kurauchi, O. Kamigaito, J. Polym. Sci. Polym. Chem. 31 (1993) 2493.
[29] P.B. Messersmith, S.I. Stupp, J. Mater. Res. 7 (1992) 2599.
[30] Y. Kojima, A. Usuki, M. Kawasumi, A. Okada, T. Kurauchi, O. Kamigaito, J. Polym. Sci. Polym. Chem. 31 (1993) 983.
[31] R. Krishnamoorti, R.A. Vaia, E.P. Giannelis, Chem. Mater. 8 (1996) 1728.
[32] H.Z. Shi, T. Lan, T.J. Pinnavaia, Chem. Mater. 8 (1996) 1584.
[33] Z. Wang, T.J. Pinnavaia, Chem. Mater. 10 (1998) 3769.
[34] Z. Wang, T.J. Pinnavaia, Chem. Mater. 10 (1998) 1820.
[35] S.D. Burnside, E.P. Giannelis, Chem. Mater. 7 (1995) 1597.
[36] P. Aranda, E. Ruizhitzky, Chem. Mater. 4 (1992) 1395.
[37] R.A. Vaia, S. Vasudevan, W. Krawiec, L.G. Scanlon, E.P. Giannelis, Adv. Mater. 7 (1995) 154.
[38] B. Liao, M. Song, H.J. Liang, Y.X. Pang, Polymer 42 (2001) 10007.
[39] M. Okamoto, S. Morita, T. Kotaka, Polymer 42 (2001) 2685.
[40] M. Riley, P.S. Fedkiw, S.A. Khan, J. Electrochem. Soc. 149 (2002) A667.
[41] G.J. Moore, M.S. Whittingham, Mater. Res. Soc. Symp. Proc. 548 (1999) 173.
[42] H.W. Chen, F.C. Chang, Polymer 42 (2001) 9763.
[43] J.J. Hwang, H.J. Liu, Macromolecules 35 (2002) 7314.
[44] D.R. Sadoway, B.Y. Huang, P.E. Trapa, P.P. Soo, P. Bannerjee, A.M. Mayes, J. Power Sources 97 (8) (2001) 621.
[45] H. Van Olphen, An Introduction to Clay Colloid Chemistry, Interscience Publishers, New York, 1963.
[46] J.D. Rhoades, Cation Exchange Capacity, vol. 2, American Society of Agronomy, Madison, WI, 1982.
[47] D.S. Ross, Recommended Methods for Determining Soil Cation Exchange Capacity, vol. 2, Northeastern Regional Publication No. 493 Revised, University of Delaware Experimental Station, Newark, DE, 1995.
[48] G.W. Thomas, Exchangeable Cations, vol. 2, American Society of Agronomy, Madison, WI, 1982.
[49] D.M. Moore, R.C. Reynolds Jr., X-ray Diffraction and the Identification and Analysis of Clay Minerals, Oxford University Press, New York, 1997.
[50] P. Aranda, E. Ruiz-Hitzky, Appl. Clay Sci. 15 (1999) 119.
[51] E. Ruizhitzky, P. Aranda, Adv. Mater. 2 (1990) 545.
[52] P. Aranda, E. Ruizhitzky, Acta Polym. 45 (1994) 59.
[53] J.H. Wu, M.M. Lerner, Chem. Mater. 5 (1993) 835.
[54] N. Ogata, S. Kawakage, T. Ogihara, Polymer 38 (1997) 5115.
[55] Z.Q. Shen, G.P. Simon, Y.B. Cheng, Eur. Polym. J. 39 (2003) 1917.
[56] F. Yan, P. Dejardin, Y. Frere, P. Gramain, Makromol. Chem. 191 (1990) 1197.
[57] R.G. Larson, The Structure and Rheology of Complex Fluids, Oxford University Press, New York, 1999.